Mathematical Biosciences and Engineering

http://www.aimspress.com/journal/mbe

MBE, 20(6): 10464–10478.
DOI: 10.3934/mbe.2023461
Received: 18 December 2022
Revised: 15 March 2023
Accepted: 30 March 2023
Published: 07 April 2023

Research article

Nonlinear neural networks adaptive control for a class of fractional-order tuberculosis model

Na Pang*

Department of Information and Computing Sciences, Xinhua College of Ningxia University, Yinchuan 750021, China

* **Correspondence:** Email: pangna234600@163.com.

Abstract: The problem of nonlinear adaptive control for a class of fractional-order tuberculosis (TB) model is studied in this paper. By analyzing the transmission mechanism of TB and the characteristics of fractional calculus, a fractional-order TB dynamical model is established with media coverage and treatment as control variables. With the help of universal approximation principle of radial basis function neural networks and the positive invariant set of established TB model, the expressions of control variables are designed and the stability of error model is analyzed. Thus, the adaptive control method can guarantee that the number of susceptible and infected individuals can be kept close to the corresponding control targets. Finally, the designed control variables are illustrated by numerical examples. The results indicate that the proposed adaptive controllers can effectively control the established TB model and ensure the stability of controlled model, and two control measures can protect more people from tuberculosis infection.

Keywords: fractional-order tuberculosis model; adaptive control; media coverage; treatment

1. Introduction

TB is a deadly infectious disease and one of the world's top ten causes of death [1–3]. Most of the infected individuals can be cured by adopting a systematical diagnostic and using appropriate antibiotics. However, the impact of TB on human health and social development still cannot be ignored due to the lack of knowledge about TB prevention and diagnosis and the low treatment coverage in some areas. According to the global tuberculosis report 2021 published by the World Health Organization [4], about 9.9 million people worldwide suffered from TB in 2020, of which more than 1.3 million died. The massive destruction caused by TB to the economy and society forces us to understand the transmission mechanism of TB deeply.

Mathematical models play an essential role in understanding the dynamics of infectious diseases,

including TB [5–10]. Exploring the transmission mechanism of tuberculosis is the first step to establishing a mathematical model, so references [11–13] have studied the transmission dynamics of tuberculosis. In addition, Castillo-Chavez and Feng [14] formulated one-strain and two-strain TB models to analyze the effects of fundamental epidemiological factors. Subsequently, the TB compartment model was proposed by Feng et al. [15] and is considered one of the basic frameworks of the transmission mechanism of TB. The authors in [16] established the TB models with fast and slow dynamics by considering multi-level contact structure. Castillo-Chavez and Song [17] comprehensively summarized the research trends of the tuberculosis dynamic models and control problems in the past decades, and proposed some exciting and challenging questions. It should be pointed out that the research results of [15] indicate that it is not enough to reduce the basic reproduction number to less than 1 for the prevention and control of TB. After that, the researchers further discussed the influence of various factors on the transmission of TB by proposing different dynamical models [18–25]. For example, Hattaf et al. [23] established a TB disease model with exogenous reinfection, and studied the optimal control problem to reduce the infectious group by using Pontryagin's maximum principle. The multi-drug resistance, and case detection and treatment were considered in [24] and [25], respectively. Meanwhile, based on the actual infection data of TB in the United States from 1988 to 2019, the authors in [26] established an SVEITR dynamical model by considering vaccination, incomplete treatment and relapse, and analyzed the sensitivity of basic reproduction number and solved the optimal control problem issue by using Pontryagin's maximum principle.

It should be pointed out that the models in all of the literature mentioned above are established by using the conventional integer-order calculus, which is a local concept. Fractional-order calculus, as an extension of integer-order one, is a global concept that can more effectively characterize the hereditary and memory properties of many physical processes and materials [27, 28]. Therefore, some scholars try to describe the spread and outbreak of infectious disease by using the fractional dynamics model [29–34]. The results show that the fractional order model can better fit the actual data. Although the fractional-order model has the above advantages, the control of the fractional TB model is still in the ascendant due to less application of fractional calculus in biology, which is one of the motivations of the current paper.

Adaptive control is one of the important control methods in engineering [35, 36]. Its characteristic is that the control target can be given in advance, and then the control variable can be designed so that the state variable or the related variable of the model can track the control target with small errors, so as to realize the control of the model. Recently, some results adopt the adaptive control method to realize the control of biology [37–39]. In particular, the authors in [39] studied the nonlinear adaptive control of COVID-19. However, the system parameters are estimated by the adaptive laws in [37–39], which are heavily dependent on the initial values of adaptive laws. Therefore, how to reduce this dependency is also one of the motivations of this paper.

Motivated by the above discussions, the problem of nonlinear neural networks control is studied for the fractional-order TB model. The main contributions of this paper are summarized as follows: (i) By analyzing the transmission mechanism of TB and considering the historical dependence on the spreading of TB, a fractional-order TB model under Caputo fractional derivative is established. Compared with the model in [33], in this paper we consider that the proportion of smear-positive and smear-negative from susceptible population is not equal to that from latent population, and the patients after rehabilitation may become susceptible ones again. (ii) This is a successful attempt to apply the

universal approximation principle of radial basis function neural networks to biological model, and thus the controllers for fractional-order TB model are proposed and the initial values dependency of adaptive laws are also reduced. Different from [37–39], where the model parameters are estimated by adaptive laws, the unknown functions that include model parameters are approximated in this paper, and thus the processes of estimations to model parameters are avoided.

This paper is organized as follows. The problem to be studied is formulated and some preliminaries are presented in Section 2. The adaptive neural networks controllers are designed and the stability of controlled model is also analyzed in Section 3. Some numerical examples are given in Section 4 to illustrate the proposed controllers. Finally, a brief summary is presented in Section 5.

2. Preliminaries and problem formulation

2.1. Preliminaries

Definition 1. [40] The Caputo derivative of function $f(t) \in C^{n+1}([t_0, +\infty), \mathbb{R})$ with the order α is given as follows

$$\mathcal{D}^{\alpha} f(t) = \frac{1}{\Gamma(n-\alpha)} \int_{t_0}^{t} \frac{f^{(n)}(\tau)}{(t-\tau)^{\alpha+1-n}} d\tau,$$

where $\Gamma(\cdot)$ denotes Gamma function, $n \in \mathbb{N}_+$ and $n-1 < \alpha \leq n$.

Definition 2. [40] For $\alpha > 0$, the Mittag-Leffler function with a single parameter is defined as $E_{\alpha}(z) = \sum_{i=0}^{\infty} \frac{z^i}{\Gamma(\alpha i+1)}$, where z is plural. In particular, $E_1(z) = e^z$.

Lemma 1. *[40] Let the function $f(t) \in C^1([t_0, +\infty), \mathbb{R})$, then $\mathcal{D}^{\alpha} f^2(t) \leq 2f(t)\mathcal{D}^{\alpha} f(t)$ for $t \geq t_0$ and $\alpha \in (0, 1]$.*

Lemma 2. *Consider the system $\mathcal{D}^{\alpha} x(t) = \varphi(t) - x(t)$ with initial value $x(0) > 0$. If $0 < \alpha < 1$ and function $\varphi(t)(t \geq 0)$ is a non-negative and bounded continuous function, then the solution $x(t)$ of this system is positive and bounded.*

Proof. This Lemma can be proven by using the similar method in [44, Lemma 5], so we omit it here. □

Lemma 3. *[41] For a given approximation accuracy $\tilde{\epsilon} > 0$, any continuous function $f(x)$ defined on a compact set can be approximated by the radial basis function neural networks $W^{*T}\Psi(x)$ as follows*

$$f(x) = W^{*T}\Psi(x) + \epsilon(x), \quad |\epsilon(x)| \leq \tilde{\epsilon},$$

where $W^* = \arg\min_W [\sup_x |f(x) - W^T\Psi(x)|]$, x represents the input vector, $W^* = (w_1, \cdots, w_l)^T \in \mathbb{R}^l$ denotes the ideal weight vector, $l > 1$ represents the nodes number, $\Psi(x) = (\Psi_1(x), \cdots, \Psi_l(x))^T$, $\Psi_i(x)$ is selected as $\Psi_i(x) = \exp[-(x-\sigma_i)^T(x-\sigma_i)/\kappa^2]$ for $i = 1, \cdots, l$, where $\sigma_i = (\sigma_{i1}, \cdots, \sigma_{in})^T$ and κ are the center and width of the Gaussian function, respectively.

2.2. Problem formulation

Since it usually takes four to eight weeks from the time TB enters the body to the time it shows symptoms, and people with TB can have either smear positive or smear negative. Therefore, the people

carrying mycobacterium TB is divided into latent population (E), smear positive population (I_1) and smear negative population (I_2). The rest of the population is classified as susceptible (S) and immune or quarantined due to cure (R). Based on the above division, literature [33] established a dynamic model of TB, discussed the global stability of disease-free equilibrium point and endemic equilibrium point, and analyzed the impact of smear-negative individuals on TB transmission. Considering that the proportion of smear-positive and smear-negative from S is not equal to that from E, and the patients after rehabilitation may become susceptible ones again, we improve the model in [33] to the following one

$$\begin{cases} \dot{S}(t) = \Pi - (\beta_1 I_1 + \beta_2 I_2)S - \mu S + \lambda R, \\ \dot{E}(t) = (1-k)(\beta_1 I_1 + \beta_2 I_2)S - (\mu + m)E, \\ \dot{I}_1(t) = p_1 k(\beta_1 I_1 + \beta_2 I_2)S + q_1 mE - (\gamma_1 + \delta_1 + \mu)I_1, \\ \dot{I}_2(t) = p_2 k(\beta_1 I_1 + \beta_2 I_2)S + q_2 mE - (\gamma_2 + \delta_2 + \mu)I_2, \\ \dot{R}(t) = \gamma_1 I_1 + \gamma_2 I_2 - (\mu + \lambda)R, \end{cases} \tag{2.1}$$

where Π represents the input rate of the population, β_1 and β_2 represent the infection rates of smear positive and negative population to susceptible population respectively, μ represents the natural mortality rate, γ_1 and γ_2 are the cure rates of smear positive and negative population respectively, δ_1 and δ_2 are the disease-related death rates of smear positive and negative infected persons respectively, λ denotes the transfer rate of the immune or quarantined population that loses immunity or released from quarantine and becomes susceptible again, m represents the transfer rate from latent population to infected population, k represents the proportion of susceptible people who become infected directly after carrying TB bacteria (p_1 and p_2 represent the proportion of smear positive and negative respectively), q_1 and q_2 represent the proportion of smear positive and negative respectively in the people who enter the infected population from the latent population. All parameters in model (2.1) are positive except $0 \leq p_1, p_2, q_1, q_2 \leq 1$ and $p_1 + p_2 = q_1 + q_2 = 1$. The initial values of model (2.1) are $S(0) > 0, E(0) > 0, I_1(0) > 0, I_2(0) > 0, R(0) > 0$.

In practice, the infection rate of the bacteria and the transfer rate of the population among the compartments depend on the infection rate and transfer rate at each historical moment. That is, it has heritability and memory, which is completely ignored by the integer-order derivative adopted in model (2.1). It is worth noting that the fractional-order derivatives can better describe the genetic and memory characteristics of the process or materials, so the fractional-order compartmental model can be established to better describe the transmission process of mycobacterium TB bacteria in the population based on model (2.1). On the other hand, effective and feasible control measures need to be taken to control the spread of the bacteria in the population. Usually, media coverage for susceptible population to reduce the infection rate and treatment for infected population are the two most commonly used control measures, which are introduced into the fractional-order compartmental model to obtain the

following fractional-order control model

$$\begin{cases} \mathcal{D}^{\alpha}S(t) = \Pi - (\beta_1 I_1 + \beta_2 I_2)S(1 - c_1u_1) - \mu S + \lambda R, \\ \mathcal{D}^{\alpha}E(t) = (1-k)(\beta_1 I_1 + \beta_2 I_2)S(1 - c_1u_1) - (\mu + m)E, \\ \mathcal{D}^{\alpha}I_1(t) = p_1k(\beta_1 I_1 + \beta_2 I_2)S(1 - c_1u_1) + q_1mE - (\gamma_1 + \delta_1 + \mu)I_1 - \dfrac{c_2u_2I_1}{1 + \alpha_1 I_1}, \\ \mathcal{D}^{\alpha}I_2(t) = p_2k(\beta_1 I_1 + \beta_2 I_2)S(1 - c_1u_1) + q_2mE - (\gamma_2 + \delta_2 + \mu)I_2 - \dfrac{c_3u_3I_2}{1 + \alpha_2 I_2}, \\ \mathcal{D}^{\alpha}R(t) = \gamma_1 I_1 + \gamma_2 I_2 + \dfrac{c_2u_2I_1}{1 + \alpha_1 I_1} + \dfrac{c_3u_3I_2}{1 + \alpha_2 I_2} - (\mu + \lambda)R, \end{cases} \tag{2.2}$$

where $\alpha \in (0, 1)$, $c_1, c_2, c_3 \in [0, 1]$ are the effective rate of control measures, $u_1, u_2, u_3 \in [0, 1]$ denote the intensity of control measures, $\alpha_1, \alpha_2 > 0$ are half-satiation constants. The reasons why we set $u_1(t), u_2(t), u_3(t)$ as control variables are summarized as follows:

(i) Media coverage for susceptible population (u_1): after the media coverage to susceptible population, people can take scientific and effective protective measures to reduce the infection rate of the bacteria, which is described by $(1 - c_1u_1)$ in (2.2).
(ii) Treatment to smear positive infected population (u_2) and smear negative infected population (u_3): due to the limited medical resources, the saturation treatment rate is used to characterize the treatment control measures.

Remark 1. *In references [29–32], fractional-order TB models were established by considering different factors that influence the transmission of TB, where the fractional derivatives with nonsingular kernel were adopted, while the Caputo fractional derivative is used in model* (2.2)*. Although the Caputo fractional derivative contains a singular kernel, this does not affect the main purpose of this paper: extend the adaptive control and neural networks approximation method widely used in the engineering fields to the biological field, and design control variables for the fractional-order TB model. It should be pointed out that the new and interesting definition of fractional derivative [27, 28, 42] proposed in recent years can effectively overcome some shortcomings of the traditional fractional derivative, but the stability theory related to these new definition is still relatively lacking, which may lead to difficulties in analyzing the stability of the controlled TB model.*

The control objectives of this paper are as follows: The appropriate expressions of u_1, u_2, u_3 in model (2.2) are designed so that the susceptible population S, smear positive population I_1 and smear negative population I_2 can track the control targets S_d, I_{1d} and I_{2d} with small errors, respectively. It is assumed that S_d, I_{1d}, I_{2d} and their fractional-order derivative with order α are all bounded and continuously differentiable. In order to achieve the control goal, the following lemma is given.

Lemma 4. $\Omega = \{(S, E, I_1, I_2, R) | S \geq 0, E \geq 0, I_1 \geq 0, I_2 \geq 0, R \geq 0, S + E + I_1 + I_2 + R \leq \frac{\Pi}{\mu}\}$ *is a positive invariant set of models* (2.1) *and* (2.2)*.*

Proof. Lemma 4 can be proved by using similar methods of [43, Theorems 1 and 2], so omitted here. □

3. Controllers design and stability analysis

In this section, the controllers are designed for the controlled model (2.2) through three steps, and then the stability of the control system is analyzed.

3.1. Design of controllers

For convenience, the control errors are defined as follows

$$\tilde{S} = S - S_d, \quad \tilde{I}_1 = I_1 - I_{1d}, \quad \tilde{I}_2 = I_2 - I_{2d}.$$

Step 1: The Lyapunov function V_1 is constructed as

$$V_1 = \frac{1}{2}\tilde{S}^2 + \frac{1}{2}\xi_1^{-1}\tilde{\theta}_1^2, \tag{3.1}$$

where $\xi_1 > 0$ is a design parameter, $\tilde{\theta}_1 = \hat{\theta}_1 - \theta_1$, $\hat{\theta}_1$ is the estimate of $\theta_1 = \|W_1^*\|^2$, W_1^* will be defined later. Based on lemma 1, the fractional-order derivative of the function V_1 is

$$\begin{aligned}\mathcal{D}^\alpha V_1 \leq & \tilde{S}\mathcal{D}^\alpha\tilde{S} + \xi_1^{-1}\tilde{\theta}_1\mathcal{D}^\alpha\tilde{\theta}_1 \\ \leq & \tilde{S}\left[\Pi - (\beta_1 I_1 + \beta_2 I_2)S(1 - c_1u_1) - \mu S + \lambda R - \mathcal{D}^\alpha S_d\right] + \xi_1^{-1}\tilde{\theta}_1\mathcal{D}^\alpha\tilde{\theta}_1 \\ = & \tilde{S}\left[c_1u_1S(\beta_1 I_1 + \beta_2 I_2) - \mathcal{D}^\alpha S_d + F_1(X_1)\right] + \xi_1^{-1}\tilde{\theta}_1\mathcal{D}^\alpha\tilde{\theta}_1,\end{aligned}$$

where $F_1(X_1) = \Pi - (\beta_1 I_1 + \beta_2 I_2)S - \mu S + \lambda R$, $X_1 = (S, I_1, I_2, R)^T$. From Lemma 4, we know that X_1 belongs to a compact set, so continuous function $F_1(X_1)$ can be approximated by radial basis function neural networks. According to Lemma 3, $F_1(X_1)$ can be approximated as $F_1(X_1) = W_1^*\Psi_1(X_1) + \epsilon_1(X_1)$, $\epsilon_1(X_1)$ is the approximation error and satisfies $|\epsilon_1(X_1)| < \tilde{\epsilon}_1$. Using Young's inequality, we get

$$\begin{aligned}\tilde{S}(W_1^*\Psi_1(X_1) + \epsilon_1(X_1)) \leq & |\tilde{S}|(\|W_1^*\|\|\Psi_1(X_1)\| + \tilde{\epsilon}_1) \\ \leq & \frac{1}{2a_1^2}\tilde{S}^2\theta_1\Psi_1^T(X_1)\Psi_1(X_1) + \frac{1}{2}a_1^2 + \frac{1}{2}\tilde{S}^2 + \frac{1}{2}\tilde{\epsilon}_1^2.\end{aligned}$$

Then, $\mathcal{D}^\alpha V_1$ can be written as

$$\mathcal{D}^\alpha V_1 \leq \tilde{S}\left[c_1u_1S(\beta_1 I_1 + \beta_2 I_2) + \frac{1}{2a_1^2}\tilde{S}\theta_1\Psi_1^T(X_1)\Psi_1(X_1) + \frac{1}{2}\tilde{S} - \mathcal{D}^\alpha S_d\right] + \frac{1}{2}a_1^2 + \frac{1}{2}\tilde{\epsilon}_1^2 + \xi_1^{-1}\tilde{\theta}_1\mathcal{D}^\alpha\tilde{\theta}_1. \tag{3.2}$$

The controller u_1 and $\mathcal{D}^\alpha\hat{\theta}_1$ are designed as

$$u_1 = \frac{1}{c_1S(\beta_1 I_1 + \beta_2 I_2)}\left[-(\rho_1 + 0.5)\tilde{S} - \frac{1}{2a_1^2}\tilde{S}\hat{\theta}_1\Psi_1^T(X_1)\Psi_1(X_1) + \mathcal{D}^\alpha S_d\right], \tag{3.3}$$

$$\mathcal{D}^\alpha\hat{\theta}_1 = \frac{\xi_1}{2a_1^2}\tilde{S}^2\Psi_1^T(X_1)\Psi_1(X_1) - \hat{\theta}_1, \tag{3.4}$$

where $\rho_1 > 0$ is a design parameter. By substituting (3.3) and (3.4) into (3.2) and noting that $\tilde{\theta}_1 = \hat{\theta}_1 - \theta_1$, we can obtain

$$\mathcal{D}^\alpha V_1 \leq -\rho_1\tilde{S}^2 - \xi_1^{-1}\tilde{\theta}_1\hat{\theta}_1 + \frac{1}{2}a_1^2 + \frac{1}{2}\tilde{\epsilon}_1^2.$$

Further, since $-\tilde{\theta}_1\hat{\theta}_1 = -\tilde{\theta}_1^2 - \tilde{\theta}_1\theta_1 \leq -\frac{1}{2}\tilde{\theta}_1^2 + \frac{1}{2}\theta_1^2$, we get

$$\mathcal{D}^\alpha V_1 \leq -\rho_1 \tilde{S}^2 - \frac{1}{2}\xi_1^{-1}\tilde{\theta}_1^2 + \Delta_1, \tag{3.5}$$

where $\Delta_1 = \frac{1}{2}\xi_1^{-1}\theta_1^2 + \frac{1}{2}a_1^2 + \frac{1}{2}\tilde{\epsilon}_1^2$.

Step 2: The Lyapunov function V_2 is constructed as

$$V_2 = \frac{1}{2}\tilde{I}_1^2 + \frac{1}{2}\xi_2^{-1}\tilde{\theta}_2^2, \tag{3.6}$$

where $\xi_2 > 0$ is a design parameter, $\tilde{\theta}_2 = \hat{\theta}_2 - \theta_2$, $\hat{\theta}_2$ is the estimate of $\theta_2 = \|W_2^*\|^2$, W_2^* will be defined later. Applying Young's inequality and noticing that $u_1 \in [0, 1]$, we can obtain

$$\begin{aligned} \tilde{I}_1 p_1 k(\beta_1 I_1 + \beta_2 I_2)S(1 - u_1) \leq & \frac{1}{2}\tilde{I}_1^2 + p_1^2 k^2(\beta_1 I_1 + \beta_2 I_2)^2 S^2 + \frac{1}{2}(1 - u_1)^2 \\ \leq & \frac{1}{2}\tilde{I}_1^2 + p_1^2 k^2(\beta_1 I_1 + \beta_2 I_2)^2 S^2 + \frac{1}{2}. \end{aligned} \tag{3.7}$$

According to Lemma 1 and using (3.7), we can easily obtain

$$\mathcal{D}^\alpha V_2 \leq \tilde{I}_1\Big[- \frac{c_1 u_2 I_1}{1 + \alpha_1 I_1} - \mathcal{D}^\alpha I_{1d} + F_2(X_2)\Big] + \xi_2^{-1}\tilde{\theta}_2\mathcal{D}^\alpha\tilde{\theta}_2 + \frac{1}{2},$$

where $F_2(X_2) = \frac{1}{2}\tilde{I}_1 p_1^2 k^2(\beta_1 I_1 + \beta_2 I_2)^2 S^2 + q_1 mE - (\gamma_1 + \delta_1 + \mu)I_1$, $X_2 = (S, E, I_1, I_2, I_{1d})^T$. The function $F_2(X_2)$ can be approximated by radial basis function neural networks because it is continuous and X_2 belongs to a compact set. According to Lemma 3, $F_2(X_2)$ can be approximated as $F_2(X_2) = W_2^*\Psi_2(X_2) + \epsilon_2(X_2)$, where $|\epsilon_2(X_2)| < \tilde{\epsilon}_2$ is the approximation error. Using Young's inequality, we get

$$\tilde{I}_1 F_2(X_2) \leq |\tilde{I}_1|(\|W_2^*\|\|\Psi_2(X_2)\| + \tilde{\epsilon}_2) \leq \frac{1}{2a_2^2}\tilde{I}_1^2\theta_2\Psi_2^T(X_2)\Psi_2(X_2) + \frac{1}{2}a_2^2 + \frac{1}{2}\tilde{I}_1^2 + \frac{1}{2}\tilde{\epsilon}_2^2,$$

where $a_2 > 0$ is a constant. Then, we have

$$\mathcal{D}^\alpha V_2 \leq \tilde{I}_1\Big[- \frac{c_1 u_2 I_2}{1 + \alpha_1 I_1} - \mathcal{D}^\alpha I_{1d} + \frac{1}{2a_2^2}\tilde{I}_1\theta_2\Psi_2^T(X_2)\Psi_2(X_2) + \frac{1}{2}\tilde{I}_1\Big] + \xi_2^{-1}\tilde{\theta}_2\mathcal{D}^\alpha\tilde{\theta}_2 + \frac{1}{2} + \frac{1}{2}a_2^2 + \frac{1}{2}\tilde{\epsilon}_2^2.$$

Design the controller u_2 and adaptive law of $\hat{\theta}_2$ as

$$u_2 = \frac{1 + \alpha_1 I_1}{c_1 I_1}\Big[(\rho_2 + \frac{1}{2})\tilde{I}_1 + \frac{1}{2a_2^2}\tilde{I}_1\hat{\theta}_2\Psi_2^T(X_2)\Psi_2(X_2) - \mathcal{D}^\alpha I_{1d}\Big], \tag{3.8}$$

$$\mathcal{D}^\alpha\hat{\theta}_2 = \frac{\xi_2}{2a_2^2}\tilde{I}_1^2\Psi_2^T(X_2)\Psi_2(X_2) - \hat{\theta}_2, \tag{3.9}$$

where $\rho_2 > 0$ is a design parameter. Substituting (3.8), (3.9) into $\mathcal{D}^\alpha V_2$, and using $\tilde{\theta}_2 = \hat{\theta}_2 - \theta_2$ and $-\tilde{\theta}_2\hat{\theta}_2 \leq -\frac{1}{2}\tilde{\theta}_2^2 + \frac{1}{2}\theta_2^2$, we can get

$$\mathcal{D}^\alpha V_2 \leq -\rho_2\tilde{I}_1^2 - \frac{1}{2}\xi_2^{-1}\tilde{\theta}_2^2 + \Delta_2, \tag{3.10}$$

where $\Delta_2 = \frac{1}{2}\xi_2^{-1}\theta_2^2 + \frac{1}{2} + \frac{1}{2}a_2^2 + \frac{1}{2}\tilde{\epsilon}_2^2$.

Step 3: Similar to step 2, construct the Lyapunov function V_3 as

$$V_3 = \frac{1}{2}\tilde{I}_2^2 + \frac{1}{2}\xi_3^{-1}\tilde{\theta}_3^2, \tag{3.11}$$

where $\xi_3 > 0$ is a designed parameter, $\tilde{\theta}_3 = \hat{\theta}_3 - \theta_3$, $\hat{\theta}_3$ is the estimate of $\theta_3 = \|W_3^*\|^2$, W_3^* is the weight vector. Similarly, we can design u_3 and $\mathcal{D}^\alpha\hat{\theta}_3$ as

$$u_3 = \frac{1 + \alpha_2 I_2}{c_2 I_2}\Big[(\rho_3 + \frac{1}{2})\tilde{I}_2 + \frac{1}{2a_3^2}\tilde{I}_2\hat{\theta}_3\Psi_3^T(X_3)\Psi_3(X_3) - \mathcal{D}^\alpha I_{2d}\Big], \tag{3.12}$$

$$\mathcal{D}^\alpha\hat{\theta}_3 = \frac{\xi_3}{2a_3^2}\tilde{I}_2^2\Psi_3^T(X_3)\Psi_3(X_3) - \hat{\theta}_3. \tag{3.13}$$

where $\rho_3 > 0$ is a design parameter, $X_3 = (S, E, I_1, I_2, I_{2d})^T$. Using lemma 1, 3 and Young's inequality, we have

$$\mathcal{D}^\alpha V_3 \le -\rho_3\tilde{I}_2^2 - \frac{1}{2}\xi_3^{-1}\tilde{\theta}_3^2 + \Delta_3, \tag{3.14}$$

where $\Delta_3 = \frac{1}{2}\xi_3^{-1}\theta_3^2 + \frac{1}{2} + \frac{1}{2}a_3^2 + \frac{1}{2}\tilde{\epsilon}_3^2$.

Remark 2. *In previous works [37–39], the vectors to be estimated by adaptive laws were constructed by using the model parameters, with the result that the initial values of adaptive laws have an important influence on the estimated value of the parameter vector. However, in this paper, the functions that contain model parameters are approximated by neural networks, and then the norms of weight vectors are estimated by adaptive laws, so it avoids the estimations to model parameters. Thus, the initial values dependency of adaptive laws are reduced.*

3.2. Stability analysis of controlled model

Theorem 1. *For control model* (2.2)*, the designed controllers* (3.3)*,* (3.8)*,* (3.12) *and the adaptive laws* (3.4)*,* (3.9)*,* (3.13) *can ensure that S, I_1 and I_2 track the control target S_d, I_{1d} and I_{2d} with small errors, respectively. That is, the control goal can be achieved.*

Proof. According to (3.1), (3.6) and (3.11),constructing Lyapunov function as $V(t) = V_1 + V_2 + V_3$. Thus, based on (3.5), (3.10) and (3.14), we have

$$\mathcal{D}^\alpha V \le -\rho_1\tilde{S}^2 - \rho_2\tilde{I}_1^2 - \rho_3\tilde{I}_2^2 - \frac{1}{2}\sum_{i=1}^{3}\xi_i^{-1}\tilde{\theta}_i^2 + \Delta \le -\rho V + \Delta,$$

where $\rho = \min\{2\rho_1, 2\rho_2, 2\rho_3, 1\}$ and $\Delta = \Delta_1 + \Delta_2 + \Delta_3$ are positive constants. Since there is $0 \le E_\alpha(-\rho t^\alpha) < 1$ for any $t \ge 0$, according to [44, Lemma 5], it can be obtained

$$V(t) \le (V(0) - \frac{\Delta}{\rho})E_\alpha(-\rho t^\alpha) + \frac{\Delta}{\rho} \le V(0)E_\alpha(-\rho t^\alpha) + \frac{\Delta}{\rho}. \tag{3.15}$$

From the form of Lyapunov function V_1, V_2, V_3, $\lim_{t\to\infty} E_\alpha(-\rho t^\alpha) = 0$ and (3.15), the control errors $\tilde{S}$, $\tilde{I}_1$ and $\tilde{I}_2$ can enter into a small neighborhood of the origin by choosing appropriate parameters Δ and ρ. In other words, under the designed control variables, the control objective of TB model (2.2) can be achieved with small error. □

Remark 3. *According to Eqs* (3.3), (3.8) *and* (3.12)*, the values of* u_1, u_2, u_3 *will lie outside the interval* $[0, 1]$ *at some time, so, the value of* u_1, u_2, u_3 *can be adjusted as follows*

$$u_i(t) = \begin{cases} 1, & u_i(t) > 1, \\ u_i(t), & 0 \le u_i(t) \le 1, \\ 0, & u_i(t) < 0, \end{cases} \quad i = 1, 2, 3.$$

The above adjustment is reasonable, which is mainly because the restriction on the range of control variables will reduce the control effect of the model to a certain extent, but will not affect the stability of the model, which is explained as follows by taking the "Step 1" in Subsection 3.1 as an example. In fact, if u_1 *is restrict into interval* $[0, 1]$*, then based on Lemma 4 and the assumptions for* S_d *in Subsection 2.2, we can conclude that the term* $c_1u_1S(\beta_1I_1 + \beta_2I_2) + \frac{1}{2}\tilde{S}\theta_1\Psi_1^T(Z_1)\Psi_1(Z_1) + \frac{1}{2}\tilde{S} - \mathcal{D}^\alpha S_d + \rho_1\tilde{S}$ *is bounded by a positive constant* ζ_1*. Thus,* (3.2) *can be rewritten as*

$$\mathcal{D}^\alpha V_1 \le |\tilde{S}|\zeta_1 + \tilde{S}\Big[-\frac{1}{2}\tilde{S}\tilde{\theta}_1\Psi_1^T(Z_1)\Psi_1(Z_1) + \frac{1}{2}\tilde{S}\tilde{\theta}_1\Psi_1^T(Z_1)\Psi_1(Z_1) - \rho_1\tilde{S}\Big] + \frac{1}{2}a_1^2 + \frac{1}{2}\tilde{\epsilon}_1^2 + \xi_1^{-1}\tilde{\theta}_1\mathcal{D}^\alpha\tilde{\theta}_1.$$

According to Lemma 2, we know that $\hat{\theta}_1$ *is bounded and thus* $\tilde{\theta}_1 = \hat{\theta}_1 - \theta$ *is bounded, which means that* $\frac{1}{2}\tilde{S}\tilde{\theta}_1\Psi_1^T(Z_1)\Psi_1(Z_1)$ *is bounded. Further, by using the boundedness of* $\tilde{S}$*,* $\mathcal{D}^\alpha V_1$ *can be calculated as*

$$\mathcal{D}^\alpha V_1 \le -\rho_1\tilde{S}^2 - \frac{1}{2}\xi_1^{-1}\tilde{\theta}_1^2 + \zeta_2,$$

where $\zeta_2 > 0$ *is a constant. Therefore, the stability of model* (2.2) *can be ensured by using the similar argument as in Subsection 3.2. Besides, this restriction also makes it possible to use the control measures in practice, because the control input outside the interval* $[0, 1]$ *is meaningless in practice.*

Remark 4. *Although there are many TB models which were built by using different fractional derivative definitions [29–32], these studies mainly focus on the existence and uniqueness of the solution, dynamic behavior, numerical methods and so on. However, the research results on the control problem of fractional TB model using adaptive control method are relatively scarce. In this paper, we successfully designed the expressions of control variables for the model by using adaptive control method and radial basis function neural networks, and analyzed the stability of the model under control variables.*

4. Numerical simulations

This section is devoted to illustrating the theoretical results in previous section by some numerical examples.

The values of parameters in model (2.2) are chosen as: $\alpha = 0.95$, $\Pi = 1.4, \beta_1 = 5.07394 \times 10^{-3}, \beta_2 = 1.01479 \times 10^{-3}$, $\mu = 1/66, m = 0.001, k = 0.001$, $p_1 = 0.35, p_2 = 0.65$, $q_1 = 0.4, q_2 = 0.6$, $\gamma_1 = 0.2038, \gamma_2 = 0.4038$, $\delta_1 = \delta_2 = 0.22$, $c_1 = 0.7, c_2 = 0.8, c_3 = 0.7$, $\alpha_1 = 1, \alpha_2 = 1$. The designed parameters in the controllers are selected as: $\rho_1 = 250, \rho_2 = \rho_3 = 20$, $a_1 = a_3 = 1, a_2 = 2$, $\xi_1 = \xi_2 = \xi_3 = 1$. The initial values of model (2.2) and adaptive laws (3.4), (3.9) and (3.13) are $(S(0), E(0), I_1(0), I_2(0), R(0)) = (5000, 80, 40, 40, 20)$ and $(\hat{\theta}_1(0), \hat{\theta}_2(0), \hat{\theta}_3(0)) = (10^{-4}, 10^{-5}, 10^{-5})$, respectively. Finally, the desired values are

$$I_{id} = I_i(0)e^{-b_it} + r_i \int_{t-\tau}^{t} [p_ik(\beta_1I_1(w) + \beta_2I_2(w))\times$$

$$S(w)(1 - c_1u_1(w)) + q_imE(w)]dw, (i = 1, 2)$$
$$S_d = b_3 + (S(0) - b_3)e^{-b_4t},$$

where $\tau = 3, r_1 = 0.3, r_2 = 0.2, b_1 = b_2 = 0.4, b_3 = 1500, b_4 = 0.3$. The parameters in radial basis function neural networks are chosen as $\sigma_i = (-30, -20, -10, 0, 10, 20, 30)^T, \kappa = 10$.

Remark 5. *Since the number of infected people at the current time depends on the cumulative number of infected people in the recent period and the initial values, the desired values I_{1d} and I_{2d} are selected as the above forms. Thus, r_1 (or r_2) represents the proportion of people who enter I_1(or I_2) from $t-\tau$ to t and have not recovered at t; $I_1(0)e^{-b_1t}$(or $I_2(0)e^{-b_2t}$) refers to the number of patients at the initial time who have not recovered at the current time t. For susceptible populations, our goal is to try to prevent them from contracting the bacteria, that is, to keep as many people as possible in S, which can be achieve by adjusting b_3 and b_4 in S_d. So, b_3 represents the number of people who are still susceptible in the end, and b_4 means the rate from $S(0)$ to b_3.*

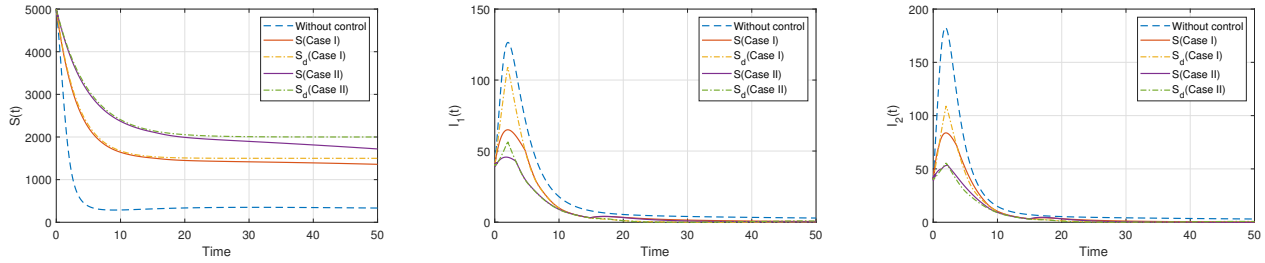

(a) (b) (c)

Figure 1. The tracking performance of S, I_1 and I_2 under different desired values.

Example 1. Tracking performance of S, I_1, I_2 to S_d, I_{1d}, I_{2d}, respectively.

As presented in Section 2, the control objective of this study is to design the controllers such that S, I_1, I_2 can track desired values S_d, I_{1d}, I_{2d} with small errors, respectively. Thus, we consider the following two cases to verify the effectiveness of the controller and the tracking performance of S, I_1, I_2 to S_d, I_{1d}, I_{2d}, respectively: Case I, $\tau = 2, r_1 = 0.3, r_2 = 0.3, b_1 = b_2 = 0.4, b_3 = 1500, b_4 = 0.3$; Case II, $\tau = 2, r_1 = 0.25, r_2 = 0.2, b_1 = 0.5, b_2 = 0.3, b_3 = 2000, b_4 = 0.2$. The main reason for choosing the

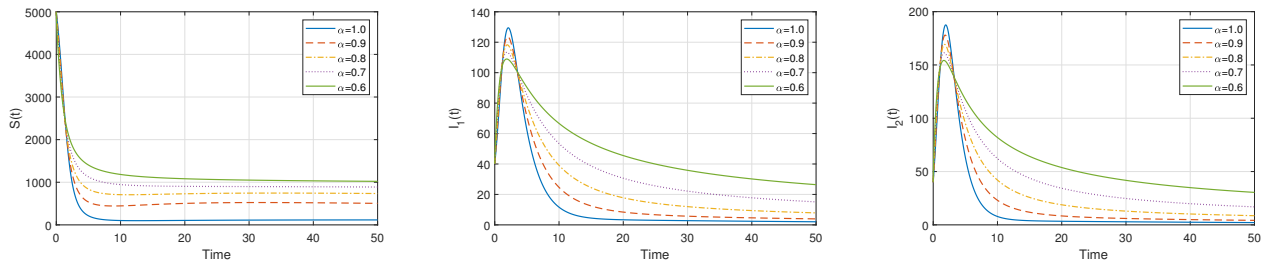

(a) (b) (c)

Figure 2. The trajectories of S, I_1 and I_2 under different α.

above parameters is that we hope that most people can change their behavior and enter the compartment R through media coverage, and most people can recover after treatment. The simulation results are presented in Figure 1. From Figure 1, we see that the trajectories of S, I_1, I_2 can track the desired values S_d, I_{1d}, I_{2d} with small errors in both Case I and II, respectively, which indicate the effectiveness of the proposed controllers. In addition, compared with the case of without control, the number of infected people decreased significantly in both Case I and II.

Example 2. The effect of the fractional-order derivative order α.

The order α is an important parameter in fractional-order model (2.2), which can be adjusted based on the actual demand. In order to exhibit the effect of α in model (2.2), we choose $\alpha = 1$ (i.e., integer-order model), $0.9, 0.8, 0.7, 0.6$, and run the numerical simulations. The results are shown in Figure 2. It can be seen from Figure 2 that with the decrease of α, the convergence speed of the trajectory of S, I_1 and I_2 are decreasing, that is, the period of TB epidemic is prolonged. This shows that the fractional-order model is more flexible than the integer-order model and has the ability to meet the needs of different situations.

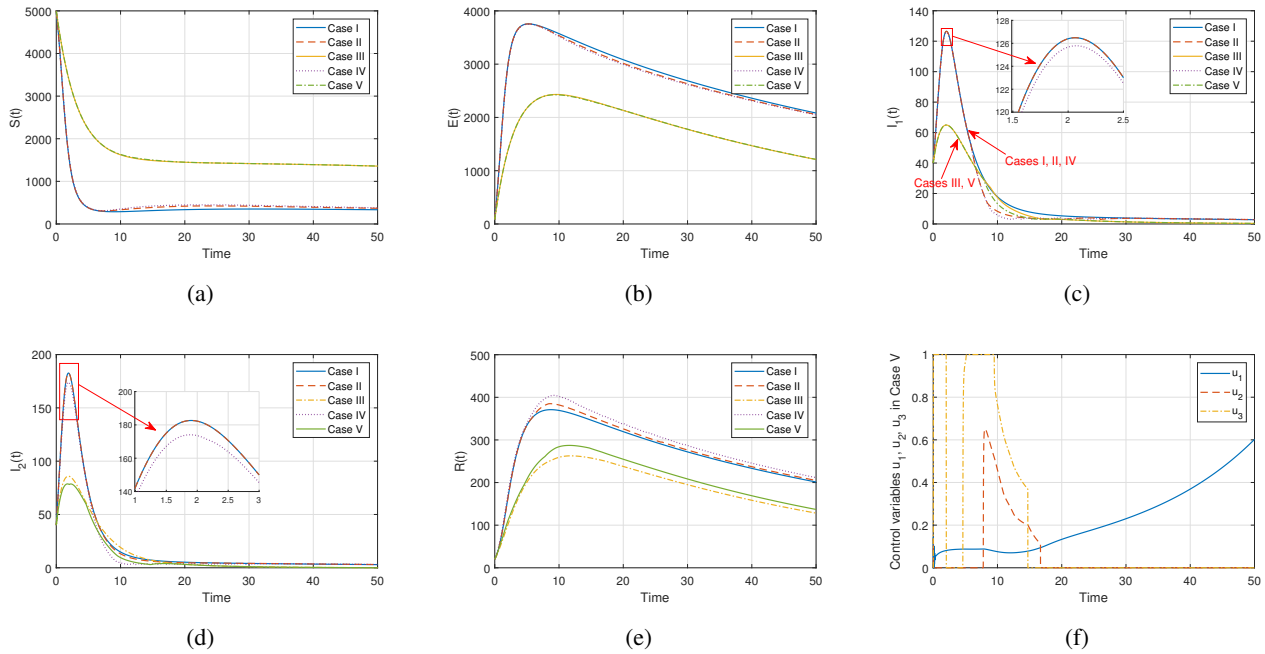

Figure 3. The trajectories of S, E, I_1, I_2, R and u_1, u_2, u_3 under different control combinations.

Example 3. The effect of different control combinations.

The purpose of setting control variables in model (2.2) is to prevent as many people as possible from contracting TB. In order to better understand the role of each control measure, we consider the following five cases: Case I, $u_1, u_2, u_3 = 0$; Case II, $u_1, u_3 = 0, u_2 \neq 0$; Case III, $u_1, u_2 \neq 0, u_3 = 0$; Case IV, $u_1 = 0, u_2, u_3 \neq 0$; Case V, $u_1, u_2, u_3 \neq 0$, where $u_i = 0$ denotes u_i is in absence, and $u_i \neq 0$ denotes that control measure u_i is adopted (this does not mean that u_i has never been equal to zero).

The simulation results are presented in Figure 3. It follows from Figure 3(a) that, compared with the cases without media coverage (i.e., Cases I, II, IV), there are more people who can remain in

compartment S when media coverage measures are taken for the susceptible people (i.e., Cases III, IV), which shows that media coverage (u_1) is an effective control measure to curb the spread of TB. Figure 3(b) shows the exposed individuals under five cases, which also indicate the significance of media coverage. From Figure 3(c),(d), we know that, when only control measures u_2 or u_3 (i.e., treatment to the smear positive and negative individuals) are adopted, their effect on reducing the number of TB infections is extremely limited. However, when media coverage and treatment measures are adopted at the same time, the infectious scale of TB epidemic can be greatly reduced. Therefore, we can conclude that comprehensive control measures can be more effective than single ones to prevent the large-scale spread of the bacteria when the TB outbreak occurs. Figure 3(e) presents the trajectories of R. The trajectories of control variables u_1, u_2 and u_3 in Case V are given in Figure 3(f).

5. Conclusions

The adaptive neural networks control problem has been investigated for the fractional-order TB model. First, based on the spreading mechanism of TB, a fractional-order compartment model of TB has been established. Then, by using the universal approximation principle of neural networks and constructing Lyapunov functions, adaptive controllers have been designed, which can ensure the control objective can be realized. Finally, some numerical simulations have been presented to illustrate the effectiveness of the proposed controllers. It should be noted that some interesting and meaningful new definitions for fractional-order derivative, including Caputo-Fabrizio, Atangana, Atangana-Baleanu, Losada-Nieto and so on [28, 42], have emerged in recent years, which, compared with Caputo derivative adopted in this paper, have nonsingular kernel. Thus, we need to consider the modeling and control problem of TB under these new definition in the future. Meanwhile, some comparisons should be made to explore the advantage and disadvantage of Caputo derivative and other new definitions, which is also one of our future works.

Acknowledgments

This work was supported by the Natural Science Foundation of China (12201330).

Conflict of interest

The author declares there is no conflicts of interest.

References

1. *Global Tuberculosis Report 2019*, World Health Organization, (2019).
2. S. Kumar, R. P. Chauhan, S. Momani, S. Hadid, A study of fractional TB model due to mycobacterium tuberculosis bacteria, *Chaos, Solitons Fractals*, **153** (2021), 111452. https://doi.org/10.1016/j.chaos.2021.111452
3. E. Barrios-Rivera, H. E. Bastidas-Santacruz, C. A. Ramirez-Bernate, O. Vasilieva, A synthesized model of tuberculosis transmission featuring treatment abandonment, *Math. Biosci. Eng.*, **19** (2022), 10882–10914. https://doi.org/10.3934/mbe.2022509

4. *Global Tuberculosis Report 2021*, World Health Organization, (2021).

5. A. Xu, Z. Wen, Y. Wang, W. Wang, Prediction of different interventions on the burden of drug-resistanttuberculosis in China: A dynamic modelling study, *J. Global Antimicrob. Resist.*, **29** (2022), 323–330. https://doi.org/10.1016/j.jgar.2022.03.018

6. X. Bai, Y. Liang, Y. Yang, J. Feng, Z. Luo, J. Zhang, et al., Potential novel markers to discriminate between active and latent tuberculosis infection in Chinese individuals, *Comp. Immunol., Microbiol. Infect. Dis.*, **44** (2016), 8–13. https://doi.org/10.1016/j.cimid.2015.11.002

7. X. Zhou, X. Shi, Stability analysis and backward bifurcation on an SEIQR epidemic model with nonlinear innate immunity, *Electron. Res. Arch.*, **30** (2022), 3481–3508. https://doi.org/10.3934/era.2022178

8. R. Haldar, S. J. Narayanan, A novel ensemble based recommendation approach using network based analysis for identification of effective drugs for Tuberculosis, *Math. Biosci. Eng.*, **19** (2021), 873–891. https://doi.org/10.21203/rs.3.rs-680480/v1

9. Z. Zhang, G. ur Rahman, J. F. Gómez-Aguilar, Dynamical aspects of a delayed epidemic model with subdivision of susceptible population and control strategies, *Chaos, Solitons Fractals*, **160** (2022), 112194. https://doi.org/10.1016/j.chaos.2022.112194

10. Y. D. Zhang, H. F. Huo, H. Xiang, Dynamics of tuberculosis with fast and slow progression and media coverage, *Math. Biosci. Eng.*, **16** (2019), 1150–1170. https://doi.org/10.3934/mbe.2019055

11. S. M. Blower, A. R. Mclean, T. C. Porco, P. M. Small, P. C. Hopewell, M. A. Sanchez, et al., The intrinsic transmission dynamics of Tuberculosis epidemics, *Nat. Med.*, **1** (1995), 815–821. https://doi.org/10.1038/nm0895-815

12. S. M. Blower, P. M. Small, P. C. Hopewell, Control strategies for Tuberculosis epidemics: New models for old problems, *Science*, **273** (1996), 497–500. https://doi.org/10.1126/science.273.5274.497

13. J. P. Aparicio, A. F. Capurro, C. Castillo-Chavez, Transmission and dynamics of Tuberculosis on generalized households, *J. Theor. Biol.*, **206** (2000), 327–341. https://doi.org/10.1006/jtbi.2000.2129

14. C. Castillo-Chavez, Z. Feng, To treat or not to treat: The case of Tuberculosis, *J. Math. Biol.*, **35** (1997), 629–656. https://doi.org/10.1007/s002850050069

15. Z. Feng, C. Castillo-Chavez, A. F. Capurro, A model for tuberculosis with exogenous reinfection, *Theor. Popul. Biol.*, **57** (2000), 235–247. https://doi.org/10.1006/tpbi.2000.1451

16. B. Song, C. Castillo-Chavez, J. P. Aparicio, Tuberculosis models with fast and slow dynamics: the role of close and casual contacts, *Math. Biosci.*, **180** (2002), 187–205. https://doi.org/10.1016/S0025-5564(02)00112-8

17. C. Castillo-Chavez, B. Song, Dynamical models of Tuberculosis and their applications, *Math. Biosci. Eng.*, **1** (2004), 361–404. https://doi.org/10.3934/mbe.2004.1.361

18. H. H. Lin, L. Wang, H. Zhang, Y. Ruan, D. P. Chinc, C. Dyed, Tuberculosis control in China: Use of modelling to develop targets and policies, *Bull. World Health Organ.*, **93** (2015), 790–798. https://doi.org/10.2471/BLT.15.154492

19. S. Liu, Y. Li, Y. Bi, Q. Huang, Mixed vaccination strategy for the control of tuberculosis: A case study in China, *Math. Biosci. Eng.*, **14** (2017), 695–708. https://doi.org/10.3934/mbe.2017039
20. Y. Cai, S. Zhao, Y. Niu, Z. Peng, K. Wang, D. He, et al., Modelling the effects of the contaminated environments on tuberculosis in Jiangsu, China, *J. Theor. Biol.*, **508** (2021), 110453. https://doi.org/10.1093/law/9780198827276.003.0047
21. E. F. D. Goufo, A. Atangana, On analysis generalization of TB-HIV dynamics by a two-scale reduction process, *Result. Phys.*, **30** (2021), 104772. https://doi.org/10.1016/j.rinp.2021.104772
22. S. Treibert, H. Brunner, M. Ehrhardt, Compartment models for vaccine effectiveness and non-specific effects for Tuberculosis, *Math. Biosci. Eng.*, **16** (2019), 7250–7298. https://doi.org/10.3934/mbe.2019364
23. K. Hattaf, M. Rachik, S. Saadi, Y. Tabit, N. Yousfi, Optimal control of tuberculosis with exogenous reinfection, *Appl. Math. Sci.*, **3** (2009), 231–240.
24. T. Yu, Y. Shi, W. Yao, Dynamic model of tuberculosis considering multi-drug resistance and their applications, *Infect. Dis. Modell.*, **3** (2018), 362–372. https://doi.org/10.1016/j.idm.2018.11.001
25. S. Athithan, M. Ghosh, Mathematical modelling of TB with the effects of case detection and treatment, *Int. J. Dyn. Control*, **1** (2013), 223–230. https://doi.org/10.1007/s40435-013-0020-2
26. Y. Li, X. Liu, Y. Yuan, J. Li, L. Wang, Global analysis of tuberculosis dynamical model and optimal control strategies based on case data in the United States, *Appl. Math. Comput.*, **422** (2022), 126983. https://doi.org/10.1016/j.amc.2022.126983
27. J. Ramadoss, A. Alharbi, K. Rajagopal, S. Boulaaras, A fractional-order discrete memristor neuron model: Nodal and network dynamics, *Electron. Res. Arch.*, **30** (2022), 3977–3992. https://doi.org/10.3934/era.2022202
28. K. Hattaf, A new generalized definition of fractional derivative with non-singular kernel, *Computation*, **8** (2020), 49. https://doi.org/10.3390/computation8020049
29. W. Shatanawi, M. S. Abdo, M. A. Abdulwasaa, K. Shah, S. K. Panchal, S. V. Kawale, et al., A fractional dynamics of tuberculosis (TB) model in the frame of generalized Atangana-Baleanu derivative, *Result. Phys.*, **29** (2021), 104739. https://doi.org/10.1016/j.rinp.2021.104739
30. Z. Zafar, S. Zaib, M. T. Hussain, C. Tunç, S. Javeed, Analysis and numerical simulation of tuberculosis model using different fractional derivatives, *Chaos Solitons Fractals*, **160** (2022), 112202. https://doi.org/10.1016/j.chaos.2022.112202
31. S. Rashid, M. K. Iqbal, A. M. Alshehri, R. Ashraf, F. Jarad, A comprehensive analysis of the stochastic fractal-fractional tuberculosis model via Mittag-Leffler kernel and white noise, *Result. Phys.*, **39** (2022), 105764. https://doi.org/10.1016/j.rinp.2022.105764
32. Adnan, S. Ahmad, A. Ullah, M. B. Riaz, A. Ali, A. Akgül, et al., Complex dynamics of multi strain TB model under nonlocal and nonsingular fractal fractional operator, *Result. Phys.*, **30** (2021), 104823. https://doi.org/10.1016/j.rinp.2021.104823
33. D. K. Das, T. K. Kar, Global dynamics of a tuberculosis model with sensitivity of the smear microscopy, *Chaos Solitons Fractals*, **146** (2021), 110879. https://doi.org/10.1016/j.chaos.2021.110879

34. K. Hattaf, On the stability and numerical scheme of fractional differential equations with application to biology, *Computation*, **10** (2022), 97. https://doi.org/10.3390/computation10060097
35. S. Wang, J. Xia, W. Sun, Observer-based adaptive event-triggered tracking control for nonlinear MIMO systems based on neural networks technique, *Neurocomputing*, **433** (2021), 71–82. https://doi.org/10.1016/j.neucom.2020.12.050
36. L. Ma, Z. Wang, C. Wang, Adaptive neural network state constrained fault-tolerant control for a class of pure-feedback systems with actuator faults, *Neurocomputing*, **490** (2022), 431–440. https://doi.org/10.1016/j.neucom.2021.12.017
37. H. Moradi, M. Sharifi, G. Vossoughi, Adaptive robust control of cancer chemotherapy in the presence ofparametric uncertainties: A comparison between three hypotheses, *Comput. Biol. Med.*, **56** (2015), 145–157. https://doi.org/10.1016/j.compbiomed.2014.11.002
38. M. H. Nematollahi, R. Vatankhah, M. Sharifi, Nonlinear adaptive control of tuberculosis with consideration of the risk of endogenous reactivation and exogenous reinfection, *J. Theor. Biol.*, **486** (2020), 110081. https://doi.org/10.1016/j.jtbi.2019.110081
39. B. Cao, T. Kang, Nonlinear adaptive control of COVID-19 with media campaigns and treatment, *Biochem. Biophys. Res. Commun.*, **555** (2021), 202–209. https://doi.org/10.1016/j.bbrc.2020.12.105
40. I. Podlubny, *Fractional Differential Equations*, Academic Press, San Diego, (1999).
41. R. M. Sanner, J. J. E. Slotine, Gaussian networks for direct adaptive control, *IEEE Trans. Neural Networks*, **3** (1992), 837–863. https://doi.org/10.1109/72.165588
42. G. S. Teodoro, J. A. T. Machado, E. C. de Oliveira, A review of definitions of fractional derivatives and other operators, *J. Comput. Phys.*, **388** (2019), 195–208. https://doi.org/10.1016/j.jcp.2019.03.008
43. H. Kheiri, M. Jafari, Fractional optimal control of an HIV/AIDS epidemic model with random testing and contact tracing, *J. Appl. Math. Comput.*, **60** (2019), 387–411. https://doi.org/10.1007/s12190-018-01219-w
44. P. Gong, W. Lan, Q. L. Han, Robust adaptive fault-tolerant consensus control for uncertain nonlinear fractional-order multiagent systems with directed topologies, *Automatica*, **117** (2020), 109011. https://doi.org/10.1016/j.automatica.2020.109011

AIMS Press